Ocean Engineering 114 (2016) 250–258

Contents lists available at ScienceDirect

Ocean Engineering

journal homepage: www.elsevier.com/locate/oceaneng

Force and torque exerted by internal solitary waves in background parabolic current on cylindrical tendon leg by numerical simulation

Haibin LÜ[a,b,c], Jieshuo Xie[a,c], Jiexin Xu[a], Zhiwu Chen[a], Tongya Liu[a,c], Shuqun Cai[a,*]

[a] State Key Laboratory of Tropical Oceanography, South China Sea Institute of Oceanology, Chinese Academy of Sciences, Guangzhou 510301, China
[b] School of Geodesy & Geomatics Engineering, Huai Hai Institute of Technology, Lianyungang 222005, China
[c] University of Chinese Academy of Sciences, Beijing 100049, China

ARTICLE INFO

Article history:
Received 28 June 2015
Accepted 25 January 2016

Keywords:
Internal solitary waves
Force
Torque
Cylindrical tendon leg
South China Sea

ABSTRACT

An internal gravity wave (IGW) model is employed to simulate the generation of internal solitary waves (ISWs) over a sill by tidal flows, and it is shown that the simulated ISW-induced current field agrees basically with that observed. Then we use this model to study the force and torque exerted by ISWs in background parabolic current on small-diameter cylindrical tendon leg of the oil platform. Eight numerical experiments are designed and the results are compared. It is found that, no matter whether a background parabolic current is considered or not, the maximum force lies at the depth of turning point (where the horizontal current in upper layer begins to turn to zero and flow against that in lower layer), a negative extremum torque appears at the depth of turning point, and the maximum torque appears at the bottom of tendon leg. With background parabolic currents, the depth of turning point becomes shallower, and the magnitude of force decreases with depth from the depth of turning point either upward or downward. In case the affecting depths of background parabolic currents are the same, both the maximum force and its appearing depth decrease with increasing current curvature. If the maximum current velocities are the same, the maximum force decreases whilst the depths of the maximum force and turning point increase with increasing current curvature. If the background current curvatures are the same, both the maximum force and its appearing depth decrease with increasing affecting depth of parabolic current.

1. Introduction

Internal solitary waves (ISWs) are usually generated by a tidal flow over variable topography in the stratified ocean, they contain enormous energy and induce strong convergence and divergence of horizontal current velocity during their propagations. ISWs are very active in the northern South China Sea (SCS, e.g., Liao et al., 2014). Strong underwater currents induced by ISWs can cause a severe threat to offshore structures (Jain, 1997; Tabeshour et al., 2006), such as the tension leg platform (TLP) in Fig. 1. The load exerted by ISWs are well studied, e.g., Cai et al. (2003; 2006; 2008a) calculate the force exerted by ISWs on piles based on Morison's empirical formula, and find that the force exerted by the first mode ISW dominates the global force which is much larger than that exerted by surface waves; Cai et al. (2014) also study the effect of a seasonal water stratification variation on the forces and torques exerted by ISWs, and find that the loads exerted by ISWs depend largely on the water stratification; Xie et al. (2010) investigate the load exerted by large-amplitude ISWs by a two-layer model based on the Miyata–Choi–Camassa equation; Zha et al. (2012) estimate the load exerted by ISWs on the cylindrical pile using nautical X-band radar observations and in-situ buoyancy frequency data; Guo et al. (2013) investigate the dynamic response of a top tensioned riser under combined excitation of ISW, surface wave and vessel motion. Moreover, numerical models are also employed for the study on load exerted by ISWs, e.g., Xie et al. (2011) compute the forces and torques associated with ISWs on a cylindrical pile based on numerical simulation; Song et al. (2011) establish a time-domain numerical model to compute the action of ISW on marine structures and their motion responses.

It is found that although the current shear has little effect on internal wave structure, the current curvature in background parabolic current could have a strong impact (Cai et al., 2008b). However, their conclusions are based on the solutions of linear internal wave modal equations, whether they are applicable to the

* Correspondence to: State Key Laboratory of Tropical Oceanography, South China Sea Institute of Oceanology, CAS, 164 West Xingang Road, 510301 Guangzhou, PR China. Tel.: +86 20 89023186.
E-mail address: caisq@scsio.ac.cn (S. Cai).

http://dx.doi.org/10.1016/j.oceaneng.2016.01.028
0029-8018/

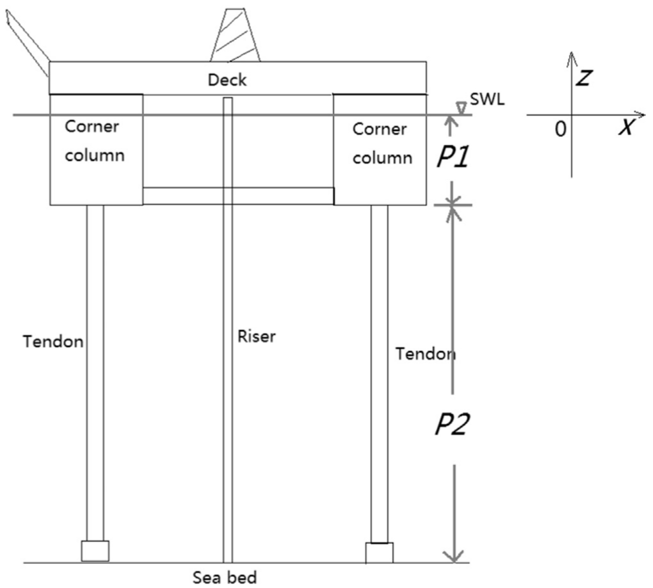

Fig. 1. A sketch of tension leg platform (▿SWL denotes the sea water level at $z=0$).

nonlinear internal solitary waves or not? This problem remains unsolved. Thus, it is natural to ask, when a background parabolic current is considered, what will happen to the load exerted by ISWs on cylindrical piles? Furthermore, what about the effect of current curvature on the load? Up to date, it seems that few numerical studies have been carried out to explain these issues.

In this paper, large amplitude ISWs generated by tidal flows over submarine topography are obtained by using an Internal Gravity Wave (IGW) model (Lamb, 2010). We mainly investigate the force and torque exerted by ISWs in different background parabolic currents on small-diameter cylindrical tendon leg of TLP. In the following, the model description, the choice of model parameters and the design of vertical background currents are described in Section 2. In Section 3, the experimental results are shown and discussed. Finally, the conclusions are summarized in Section 4.

2. Model and TLP description

2.1. Model description

We consider a two-dimensional (x, z) flow in a continuously stratified ocean of variable depth. The sea surface is at $z=0$, z is positive upward. The IGW model, a two dimensional non-hydrostatic nonlinear model, is used in this work (Lamb, 2010). This numerical model has been successfully used to study a series of ISW generation problems. Under the Boussinesq approximation, the governing equations are reduced from the incompressible Navier–Stokes equations as follows,

$$\tilde{\rho}(u_t+u\cdot\nabla u)=-\nabla\tilde{p}-\tilde{\rho}g\hat{k}+\mu\nabla^2 u \tag{1}$$

$$\tilde{\rho}_t+u\cdot\nabla\tilde{\rho}=\kappa\nabla^2\tilde{\rho} \tag{2}$$

$$\nabla\cdot u=0 \tag{3}$$

where, $\tilde{\rho}$ is the density, $\boldsymbol{u}=(u, w)$ is the velocity in the x, z-plane, g is the gravitational acceleration, $\tilde{p}$ is the pressure, κ is the diffusivity and μ is the viscosity. The equations are solved by splitting the density and pressure into two parts via

$$\tilde{\rho}=\rho_0(1+\rho) \tag{4}$$

$$\tilde{p}=-\rho_0 g z+\rho_0 p \tag{5}$$

Here, $\rho_0=1025\ \mathrm{kg\ m^{-3}}$ is a reference density, ρ is a nondimensional density from the reference density, and p is a nondimensional variation from the pressure. Details of the IGW model can be found in Lamb (2010).

The bottom topography of the ridge is defined as

$$H(x)=-[H_0-h_0\exp(-x^2/W^2)] \tag{6}$$

where $H_0=400$ m is the water depth, $h_0=270$ m is the height of ridge, and $W=15$ km is the width of ridge. The domain is sufficiently long that no perturbations reach the boundary. At the left boundary of the computational domain, the M_2 barotropic tidal flow with a maximum velocity of $U_0=0.3\ \mathrm{ms^{-1}}$ and a tidal period T of 12.4 h is prescribed, while a radiation condition is applied at the right boundary. The computational domain extends from $x=-L$ to L (here L is 300 km), and a background parabolic current $U(z)$ is only prescribed at $x<-34$ km in the initial condition. In all simulations, the horizontal spatial resolution in the domain is about 100 m, and there are 82 levels in vertical direction. To simplify the calculation, vertical viscosity, vertical diffusivity and stress at bottom are not considered. In fact, in our additional sensitive experiments, when the free-slip conditions at bottom are substituted by the non-slip conditions, there exists only a slight difference between the modeled current fields near the bottom. In the vertical direction, a sigma coordinate transformation in regard to depth is introduced. The thickness of the layer is reduced in the depth intervals with strong stratification by introducing new variables (Vlasenko and Alpers, 2005),

$$x_2=x,\ z_2=\int_z^0 N(s)ds\Big/\int_{-H(x)}^0 N(s)ds \tag{7}$$

which makes the computation more effective for the ISWs in the main thermocline. The maximum time step is 20 s, and a variable time step is used to satisfy the Courant–Friedrichs–Lewy (CFL) condition.

In the model, the vertical distribution of the nondimensional density ρ is defined by,

$$\rho(z)=\frac{-N_0^2}{g\times\left[z+25\times 50\times\left(1+\tanh\left(\frac{z+80}{50}\right)\right)\right]} \tag{8}$$

Here, we set the square of buoyancy frequency in the lower ocean $N_0^2=1.73\times 10^{-5}\ \mathrm{s^{-2}}$, so that the corresponding calculated buoyancy frequency profile $N(z)$ gets the maximum (~12.16 cph) at a depth of $z=-80$ m, and the vertical distribution of $N(z)$ shown in Fig. 2 is similar to the in-situ observational data at the observational site (21°2′N, 117°37′E) near the Dongsha Islands in the northern SCS during June 24–25, 2009. The pycnocline lower boundary is at $z=-150.5$ m denoted by the dashed line in Fig. 2, where the buoyancy frequency is defined as the half of the maximum N.

In the following, except in experiment E0 without background current, seven cases of background parabolic currents (E1–E7) are designed to study the sensitivity of the load exerted by ISWs to different background currents by comparisons: (i) with and without background parabolic currents (experiment E0 versus the other experiments); (ii) the variation of background current curvature with different maximum current velocity (experiment E1 versus E2, experiment E3 versus E4, and experiment E5 versus E6); (iii) the variation of background current curvature with different affecting depth of parabolic current (experiment E1 versus E4 or E5; experiment E2 versus E3 or E6); (iv) the variation of affecting depth of parabolic current with a same background current curvature (experiment E4 versus E7). See Table 1 and Fig. 3 for the eight experimental cases.